# Multi-disciplinary Shape Optimization of Aerostat Envelopes

C. Vijay Ram[1]
*Ashok Leyland limited, Chennai, 600035, India*

Rajkumar S. Pant[2]
*Indian Institute of Technology Bombay, Mumbai Maharashtra, 400076, India*

**This paper discusses an MDO approach for identifying the optimum shape of an aerostat envelope that results in the largest payload capacity for a given envelope volume. The participating disciplines in this optimization problem are Aerodynamics, Flight Mechanics and Structures. Constraints that take into consideration the difficulty in fabrication of certain kinds of shapes have been included. The paper starts with a description of how the aerostat envelope shape affects its payload carrying ability. Some details of a previous study on parameterization of envelope shape and optimization from aerodynamic and structural considerations alone are presented. A methodology for fin sizing from static stability considerations is presented, which includes determination of tether profile. Results of envelope shape optimization studies reveal that payload capacity can be increased by around 6.5% by using multi- fabric construction, by using lighter fabric in less stressed regions. Sensitivity analyses revealed that the payload capacity decreases considerably with increase in fabric density, and tether weight per unit length due to increased self weight, and angle of attack. It was also seen that the fin weight and the location of confluence point depend to a great extent, on the location of CG.**

## Nomenclature

| | | |
|---|---|---|
| $C_{m_\alpha}$ | = | Change in moment coefficient with angle of attack (Stability margin) |
| $S$ | = | surface area |
| $\sigma$ | = | stress |
| $C_{DV}$ | = | Volumetric Drag coefficient |
| $d_{\max}$ | = | max. diameter |
| $(\overline{x_c}, \overline{z_c})$ | = | Coefficients of confluence point |
| $P_R$ | = | Internal overpressure in the aerostat envelope |
| $d_{\max}$, $y_{\max}$ | = | max. diameter and radius of aerostat envelope, respectively |
| $t$ | = | envelope material thickness |
| R | = | Radius of curvature of spherical front portion |
| $a_1, b_1, c_1, d_1, a_2, b_2, c_2, d_2$ | = | Coefficients of cubic splines that parameterize middle portion of envelope |
| $a_n$ | = | Coefficient for parabolic rear shape |
| $\rho_{matl}$ | = | Area density (weight per unit area) of envelope material |

## I. Background and Introduction

An aerostat is an aerodynamically shaped tethered body, belonging to the family of Lighter-than-air vehicles. Aerostat envelopes are filled with a 'lighter than air' gas (which is Helium or Hydrogen in most cases) and thus generate lift due to buoyancy. The envelope is gimbaled at the tether confluence point, so that it can freely align with the direction of the ambient wind. Adequately sized fins are provided on the envelope to impart it stability during wind disturbances. Payloads in modern day aerostats are usually radars, surveillance cameras or communication equipment. In order to deploy more sophisticated equipment on Aerostats, it is always desirable to increase their payload capacity, without compromising on their operating altitude. This paper provided details of a methodology for arriving at the optimum shape of the envelope of an aerostat, keeping in mind the aerodynamic and structural considerations, while incorporating some constraints imposed from manufacturing considerations.

---

[1] Senior Engineer, Advance Engineering, Non member.
[2] Associate Professor, Aerospace Engineering Department, Powai, Member.

## II. Effect of envelope shape on an aerostat's payload capacity

The envelope shape affects the payload capacity in many ways. The envelope weight is decided by the Total Surface Area (TSA) of the envelope, which, for a given envelope volume, can vary greatly with its shape. The difference in internal and external pressure on the aerostat envelope generates stress on the membrane. For a given pressure difference, the stress is a function of the envelope shape. If the stress is low, a material of low ultimate strength can be used, which is expected to be lighter. On the other hand for a higher stress, a stronger material which is expected to be heavier (due to higher $\rho_{matl}$) will have to be used. Thus shape directly influences the self weight of the aerostat. The envelope shape also decides the aerodynamic force and moments generated on it. The size of fins required to trim the aerostat at a given angle of attack and to provide the required stability is thus a function of its shape. The ambient wind on the aerostat produces drag which tends to displace it along the direction of flow. This displacement is called blow-by, and it reduces the operational height of an aerostat and may also give rise to functional disadvantages depending on the application, for instance, to maintain the specified altitude of operation; a longer tether will have to be released at the expense of a decrease in payload capacity. To increase the payload capacity, it is thus necessary to reduce the envelope drag coefficient $C_D$.

## III. Previous study in aerostat envelope shape optimization

In a previous study by Kanikdale et al.[1], the envelope geometry of an aerostat was parameterized using a sphere for the nose, two cubic splines for the mid-body and a parabola for the rear, as shown in Figure 1.

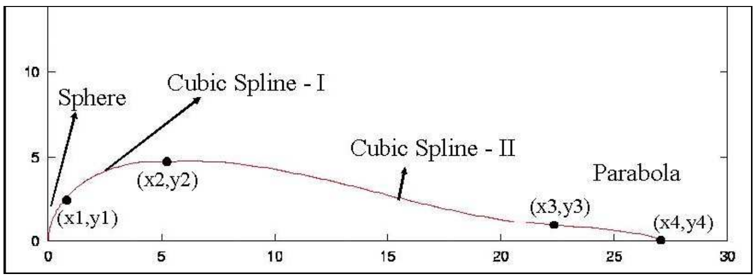


**Figure 1. Parameterization of geometry**[1]

The defining equations for the various shape segments are given in Eqns. (1-4).

Sphere (Circle in 2-D): $$y^2 = 2xR - x^2 \tag{1}$$

Spline I: $$y = a_1 x^3 + b_1 x^2 + c_1 x + d_1 \tag{2}$$

Spline II: $$y = a_2 x^3 + b_2 x^2 + c_2 x + d_2 \tag{3}$$

Parabola: $$y^2 = a_n (x_4 - x) \tag{4}$$

By imposing constraints on the slope continuity at points $(x_1, y_1)$, $(x_2, y_2)$ and $(x_3, y_3)$, and zero slope at point $(x_2, y_2)$ for an aerostat envelope of fixed volume, the size of the design vector was reduced to six, viz., $X_D = (x_1, y_2, x_2, x_3, y_3, x_4)$. Additional constraints on the radius of curvature and rate of change of slope were also employed to incorporate manufacturing constraints. A shape generation algorithm was developed, which generated various possible shapes of aerostat envelopes by varying these geometrical parameters, while meeting the specified constraints.

An objective function $F_{comp}$ incorporating the disciplines of Aerodynamics (through Volumetric Drag Coefficient $C_{DV}$), and Structures (through Envelope Surface Area S, and Max. stress $\sigma_{max}$) was formulated as:

$$F_{comp} = w_1\left(\frac{C_{DV}}{(C_{DV})_{GNVR}}\right) + w_2\left(\frac{S}{S_{GNVR}}\right) + w_3\left(\frac{\sigma \max}{\sigma_{GNVR}}\right) \tag{5}$$

Where $w_1$, $w_2$ and $w_3$ are user-specified weight functions. The subscript GNVR in the quantities listed above refer to the corresponding values of these parameters for a reference GNVR shape. The optimum shape for various values of weight functions was obtained by coupling the shape generation algorithm to an optimizer. In the present work, the GADO (Genetic Algorithm for Design Optimization) code developed by Rasheed[2] has been coupled to the shape generation algorithm to obtain the envelope shape that maximizes the payload capacity. Figure 2 shows the methodology adopted for solving the problem.

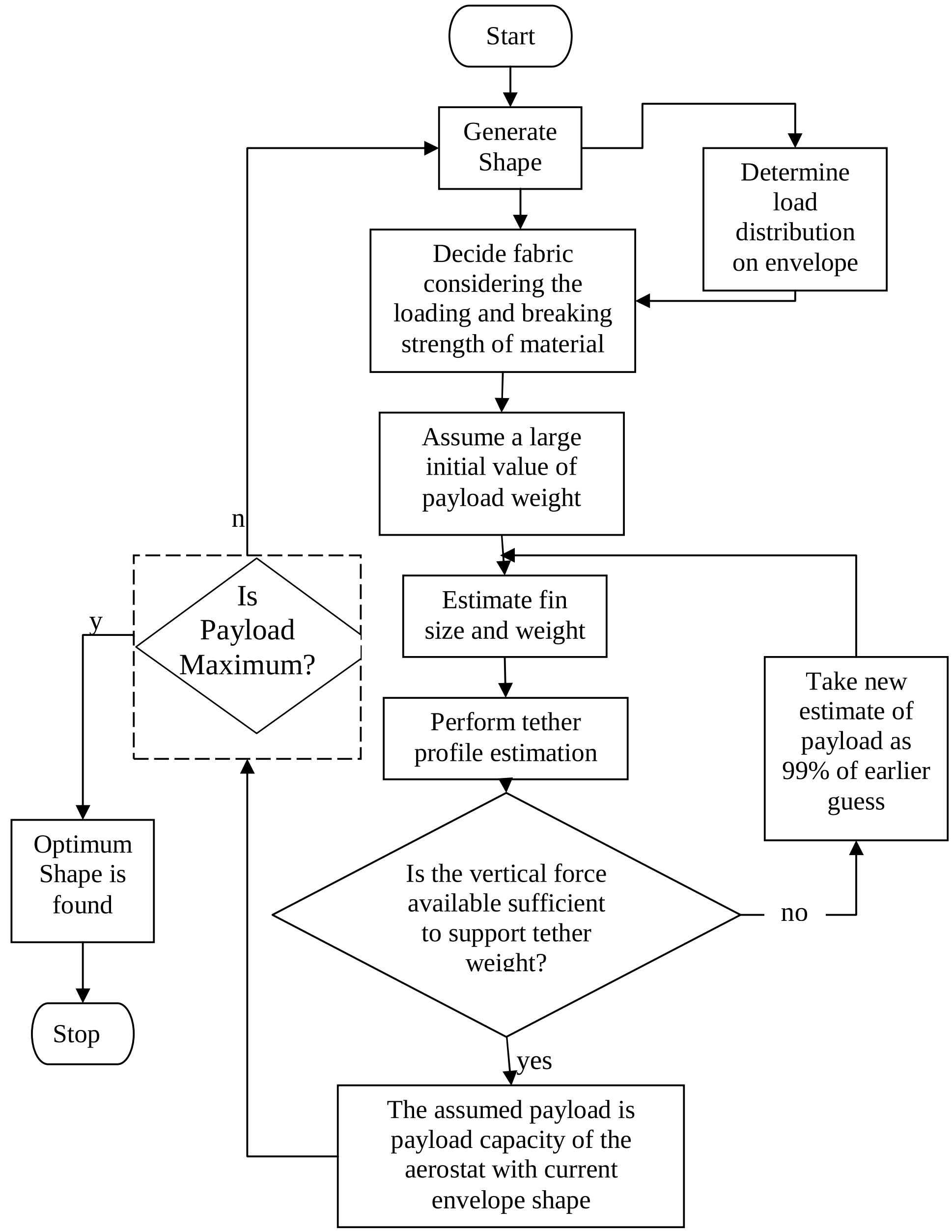


**Figure 2. Methodology for Shape Optimization**

In order to eliminate the need of using a flow solver for determination of $C_{DV}$ in every iteration of the optimization process, a co-relation between $C_{DV}$ and some geometry related parameters is required. Such an empirical formula was developed for an aerostat of envelope volume 1000 $m^3$ and a length of 26.26 m, by computing $C_{DV}$ for a number of envelope shapes. Aerodynamic analyses were carried out using FLUENT™ flow solver package. An axi-symmetric, solver was used in conjunction with S-A turbulence model. Figure 3 shows the structured grid around a trial envelope shape and the semi-circular domain that was used.

In this study, the envelope length was kept fixed to avoid compromising on stability with respect to the reference GNVR shape. However, it is a known fact that the size of the fins can be greatly reduced if the envelope length is increased, which results in a larger payload. Secondly, the formulation used in Kanikdale et. al[1]'s model was not amenable to coupling with an MDO process, since it requires detailed geometric data about the envelope shape, especially the co-ordinates of several points at the nose and trailing edge, and the grid density in these regions. The co-relation was arrived using some arbitrarily derived coefficients, purely based on observation of the flow patterns.

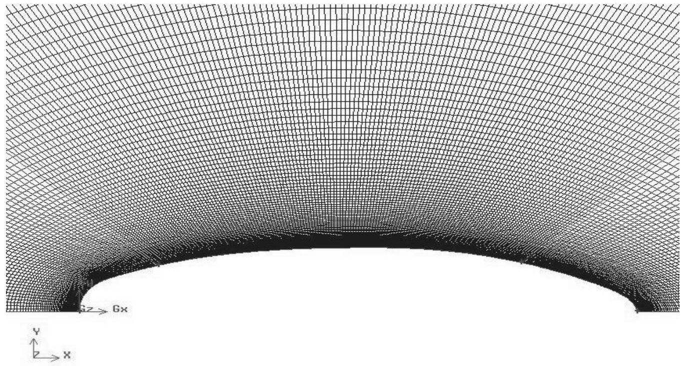

**Figure 3. Structured grid around Aerostat envelope in a semicircular domain**

## IV. Details of present study

In the present work a more generic expression[3] to estimate $C_{DV}$ is used, which is a function only of the six geometrical parameters. The problem is formulated to maximize payload. The drag on the aerostat envelope and the stresses generated are expressed in terms of the penalty that they impose on payload capacity of the aerostat. The weight of the fins required for stability is estimated to accurately predict the payload capacity. Unlike in the previous study, the length of the aerostat has also been kept as a free variable, since appropriate restrictions have been inserted on the length by requirement on the size of fin.

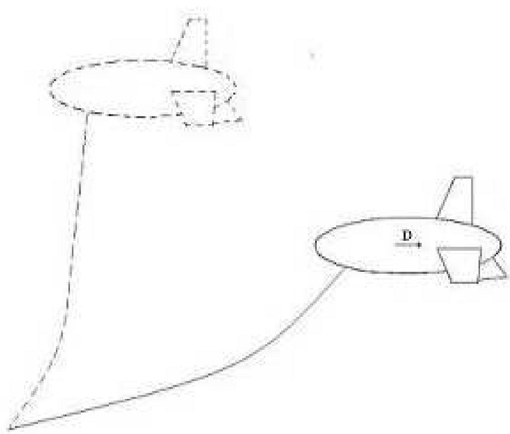


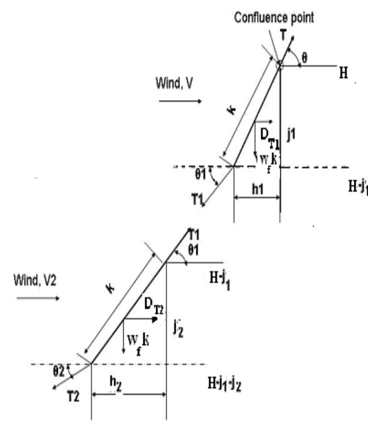


**Figure 4. Reduction in operation height due to *blowby*** **Figure 5. Forces on each tether element**

The drag on an aerostat produces *blowby* or lateral displacement, due to which either a longer tether is required to maintain a particular operational height, or there is a decrease in operational height of the aerostat, for a given tether length, as shown in Figure 4. The added weight of the tether decreases the payload capacity. To obtain a correct estimate of the payload capacity, the tether profile and weight for a given drag coefficient is obtained using the methodology suggested by Wright[4]. In this method, the tether is discretized into small elements of equal lengths, starting from the confluence point. The tension and angle of inclination of each of these elements are determined by considering the equilibrium of forces on them, as shown in Figure 5.

### A. Methodology for Sizing of Fins of an Aerostat

Fins are required for the stability of the aerostat, but they also constitute a major portion of the weight and also add to the drag. In order to accurately estimate the payload capacity of the aerostat, the size and weight of the fins that would be required for adequate stability are estimated. A methodology for sizing the inverted Y-shaped fins of a tethered aerostat has been developed, in which the stability analysis is based on the approach suggested Krishnamurthy & Panda[5]. Figure 6 shows the flow chart of this methodology.

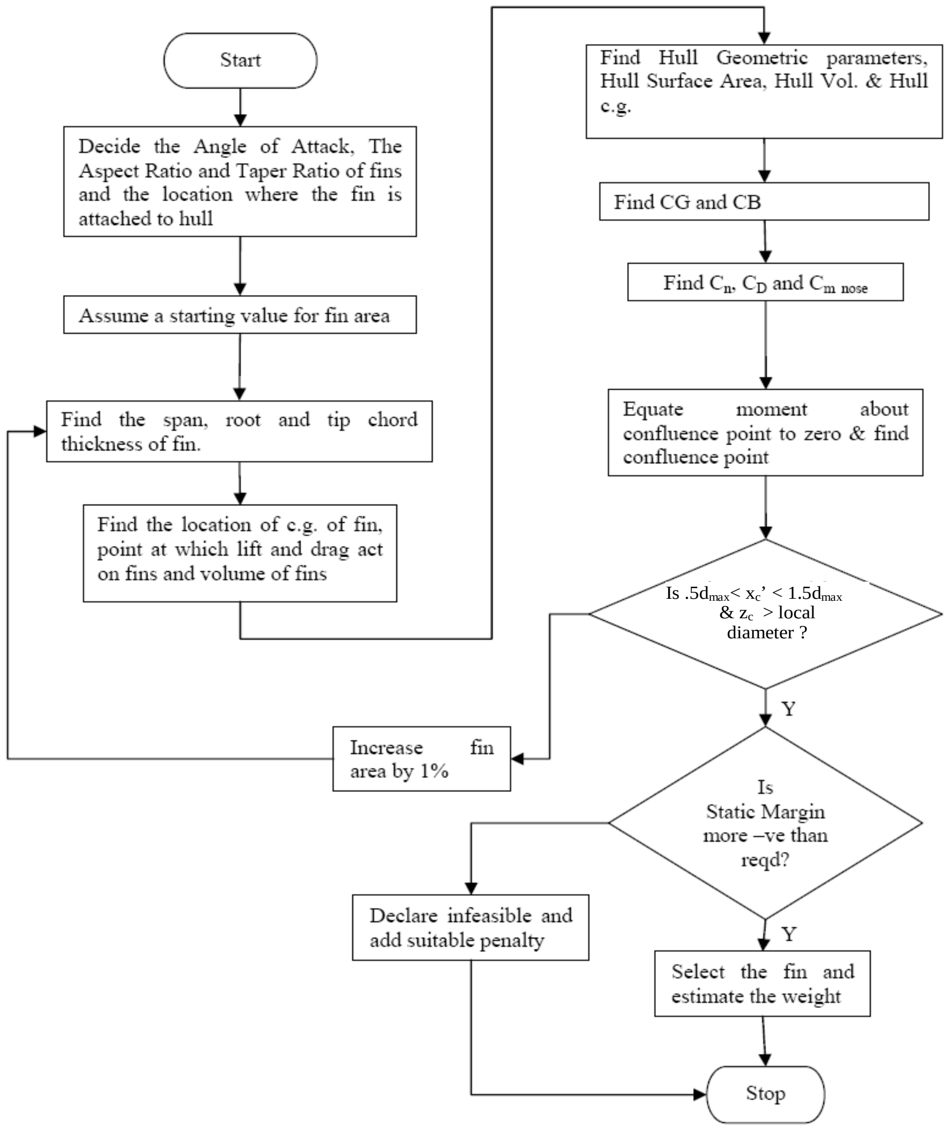


**Figure 6. Flow chart of fin sizing methodology**

An inverted Y configuration is selected for the fins so that rain and snow falling on the fins does not accumulate on the fins thus avoiding disturbance to the balance of the aerostat. The coordinates of the confluence point $(\overline{x_c}, \overline{z_c})$ for a given size of fin can be obtained and thus the stability margin $C_{m_\alpha}$ taken about the confluence point can be obtained. The aspect ratio, taper ratio and location of the fin along the hull are initially assumed. The fin area required for adequate stability is determined through an iterative process. Starting from a small initial guess, the fin area is increased till the confluence point is at an acceptable location. If the aerostat has sufficient static margin for the given fin size and confluence point, it is accepted. Empirical co-relations for aerodynamic coefficients suggested by Jones and De-Laurie[6] for symmetric fin configuration, and Malik, Gill and Pant[7] for un-symmetric Y-fin configuration are utilized in this methodology.

### B. Envelope Weight Estimation and Structural Considerations

The self-weight of the hull is estimated as a function of the weight of the envelope fabric. The weight of the fabric of the envelope depends on the surface area of the aerostat and the density of the material used. The material used for the construction of the envelope should be strong enough to withstand the loads developed due to the internal pressure of the gas inside the aerostat, and the dynamic loads imposed due to the ambient wind.

Structural considerations in the present study involve estimating the hoop and bending stress developed in the envelope.

### C. Aerostat Envelope Weight Reduction by Multi fabric Construction

In order to maximize the payload of the aerostat, the self-weight of the aerostat should be reduced to the extent possible. The load on the fabric is not uniform throughout the fabric. The hoop stress of the aerostat envelope is given by:

$$\sigma = (P_R \times y_{\max})/2t \tag{6}$$

This equation shows that regions with a larger diameter in the middle of the aerostats are more loaded and regions of smaller diameter near the ends of the aerostat are lightly loaded. Hence a great advantage in terms of payload capacity of the aerostat can be achieved if the front and rear of the aerostat are made with lighter materials of comparatively low strength and the middle regions are made with high strength (but comparatively heavier) material as shown in Figure 7 rather than using the same material for the entire aerostat.

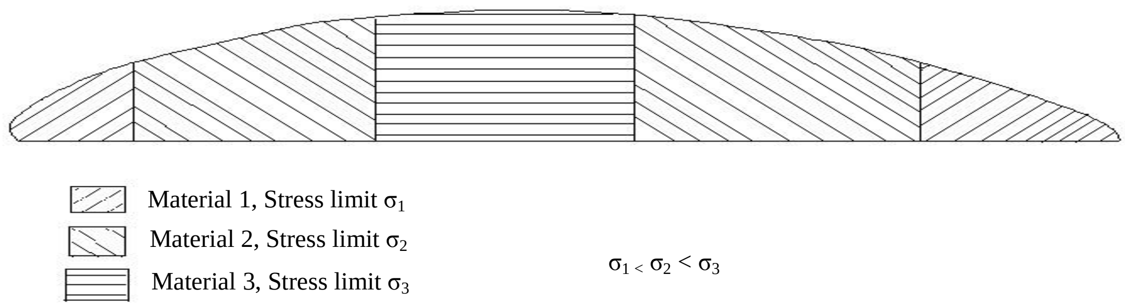


**Figure 7. Multi-fabric construction of the aerostat envelope**

The fabric to be used for each portion of the aerostat and the fabric weight of the aerostat were estimated based on the values of load acting per unit length along the meridians (warp direction) and along latitude circles (weft). Considering a suitable factor of safety, a fabric having breaking strength just higher than the tensile force developed will be used for that particular portion.

The breaking strength of a fabric is generally reported in terms of load per unit width. Typical data related to the load per unit width for three fabrics, and their respective specific weights used in this study are listed in **Error! Reference source not found.**.

**Table 1. Material Properties of aerostat fabrics**

| Properties | Fabric # 1 | Fabric # 2 | Fabric# 3 |
|---|---|---|---|
| **Specific Mass (g/m$^2$)** | 280 | 340 | 385 |
| | **Breaking Strength (kN/m)** | | |
| **Warp direction** | 15 | 30 | 45 |
| **Weft direction** | 14 | 30 | 45 |

Using this data, the envelope profile for minimum fabric weight, employing a multi fabric construction of the envelope was obtained. The shape of the envelope was optimized for minimum fabric weight using a multi fabric approach. It was found that for a factor of safety of 4, the maximum load on the material was lower than the design breaking strength for Fabric # 2. Thus, Fabric # 3 is not required for this shape. A saving of ≈ 20 kg was obtained in the fabric weight using multi fabric construction, as compared to an envelope of single fabric construction using Fabric # 1, which represents a 6.5% savings in fabric weight, which can directly be translated into increase in payload.

The methodology has been employed for an aerostat of 2000 m$^3$, and various solutions for multi-fabric envelope configurations have been obtained.

### D. Results Obtained

The payload capacity of an aerostat having a GNVR shaped envelope was estimated for a single and multiple fabric construction. The fabric distribution in the multi fabric construction is as shown in Figure 8.

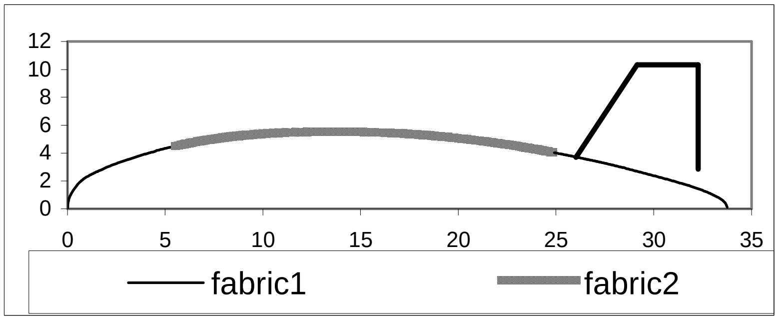


**Figure 8: Fabric distribution for multi-fabric GNVR shaped aerostat**

The weight breakup calculated for the single fabric and multi-fabric construction is given in Table 2.

**Table 2. Properties of single and multi-fabric GNVR shaped aerostats**

| Component Weight | Single fabric (kg) | Multi-fabric (Kg) |
|---|---|---|
| Payload (Kg) | 237.4 | 286.4 |
| Fin (Kg) | 107.8 | 75.4 |
| Envelope Membrane (Kg) | 309.4 | 293.6 |
| Tether Force (Kg) | 735.1 | 734.4 |
| **Location of Confluence point** | | |
| $x_c$ (from nose) (m) | 11.4 | 6.9 |
| $z_c$ (m) | 11.6 | 10.6 |

## E. Optimum Shape for Single Fabric Construction of Aerostat

The four optimum shapes of single fabric aerostats were determined using the GA based optimizer GADO are shown in Figure 9.

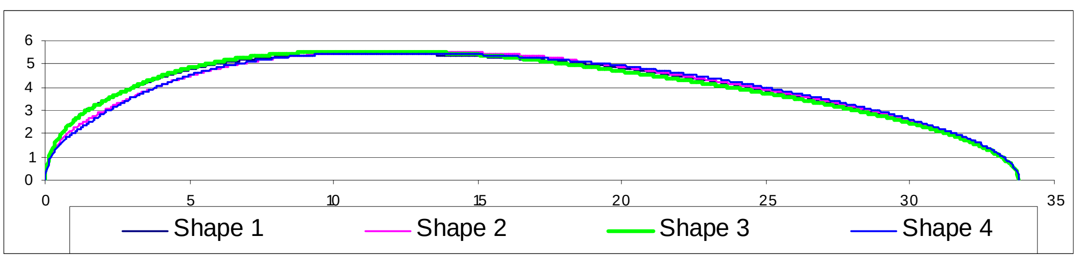


**Figure 9 Optimum shapes of single fabric aerostat envelopes**

The weight breakup of these shapes is given in Table 3. It can be seen that while all these shapes have almost the same payload carrying capacity, Shape 2 has the maximum. This shape has the least surface area, hence the least envelope weight. The low surface area also reduces the drag on the shape, hence the force required to lift the tether is also low.

**Table 3. Weight break up of single fabric Aerostats**

| Profile | Payload (Kg) | Fin (Kg) | Envelope Fabric (Kg) | Tether Force (Kg) |
|---|---|---|---|---|
| Shape 1 | 241.9 | 99.2 | 312.2 | 736.5 |
| Shape 2 | 242.5 | 102.1 | 310.5 | 734.7 |
| Shape 3 | 242.2 | 97.9 | 311.5 | 738.2 |
| Shape 4 | 240.5 | 102.4 | 310.8 | 736.1 |

The profile of the shape along with the fin is shown in Figure 10. It's confluence point is located at $x_c$'= 10.8m behind the nose and $z_c$= 11.1 m below the axis, which is an acceptable position.

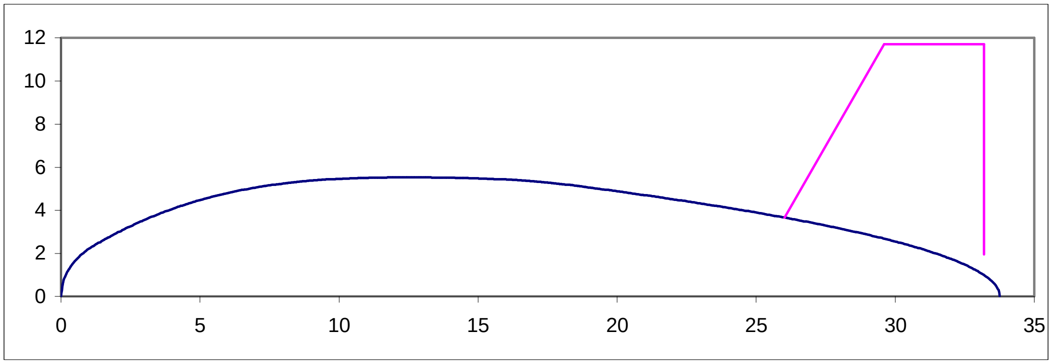


**Figure 10. Best envelope shape for single fabric construction of Aerostat**

### F. Optimum Shape for Multi Fabric Construction of Aerostat

The optimum shapes for a multi-fabric aerostat obtained from four different runs of GADO optimizer are shown in Figure 11. These shapes result in considerable reduction in weight of envelope fabric weight and fin but the confluence point is located close to the nose (as fabric distribution moves the CG backwards) which is not an acceptable position. The confluence point can however be maintained at any desired position by adjusting the position of the payload and consequently the CG of the aerostat.

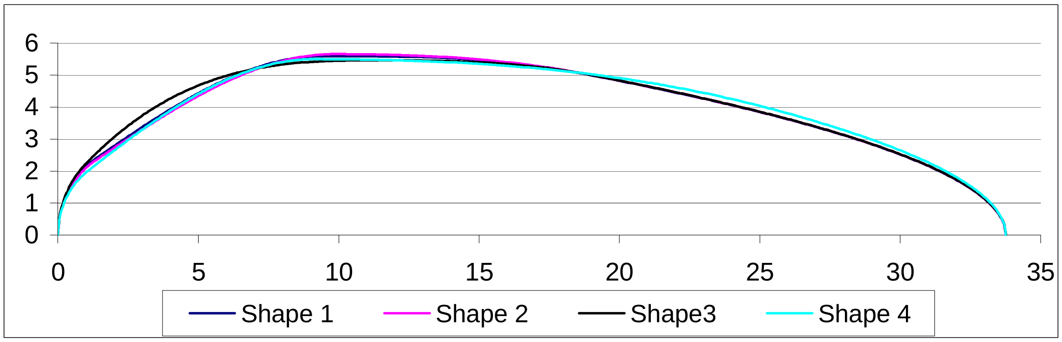


**Figure 11. Optimum shapes for multi fabric aerostats**

**Error! Reference source not found.**4 gives the weight breakup of the four different multi-fabric shapes obtained through optimization. It can be seen that while all these shapes have almost the same payload capacity, but Shape 1 has the maximum.

**Table 4. Weight Breakup for Multi Fabric Shapes**

| Profile | Payload capacity (Kg) | Envelope fabric weight (Kg) | Fin weight (Kg) | Tether force (Kg) |
|---|---|---|---|---|
| Shape 1 | 296.2 | 288.2 | 69.1 | 736.2 |
| Shape 2 | 294.3 | 290.0 | 69.3 | 736.2 |
| Shape 3 | 293.1 | 293.2 | 69.3 | 734.2 |
| Shape 4 | 295.1 | 287.2 | 69.5 | 737.9 |

The profile of this aerostat along with the fin size is shown in Figure 12. The thick jagged line shows regions in which the stronger fabric is used. The shape shown in Figure 12 has a maximum diameter of 11.2 m. The ideal position of the confluence point for this shape is $x_c$'=11.2 m behind the nose and $z_c$ = 11.2 m below the axis. By adjusting the CG of the aerostat shown, if the confluence point was brought near to the desired location, the new weight breakup and the confluence point location are as listed in **Error! Reference source not found.**5.

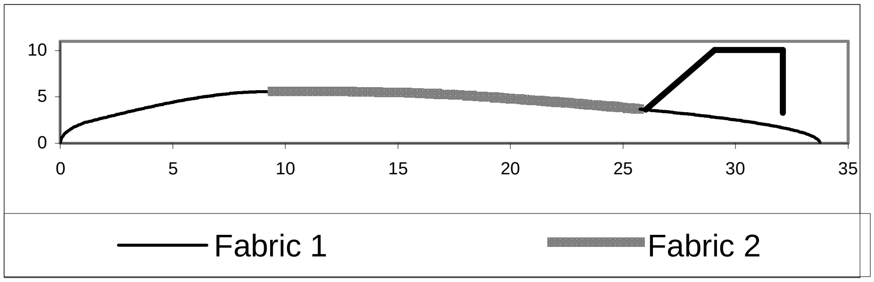


**Figure 12: Multi-fabric aerostat having highest payload capacity**

**Table 5: Multifabric envelope properties after CG adjustment**

| Payload Capacity (Kg) | Fin weight (Kg) | Fabric weight (Kg) | Tether force Kg) | $x_c$' (m) | $z_c$ (m) |
|---|---|---|---|---|---|
| 252.7 | 110 | 288.2 | 738.2 | 10.8 | 12.7 |

It can be seen that the payload capacity was still nearly 11 Kg (≈4.5%) greater than that for the most optimum single fabric envelope.

### G. Sensitivity Analyses

Sensitivity of the payload capacity of the aerostat to operating conditions and design requirements has also been studied. In all the studies, the input parameter was varied in the range of ±10% from the design condition for the most optimum single fabric aerostat (shown in Figure 8) and the effect on payload capacity studied. It was observed that payload capacity decreases considerably with increase in fabric density, and tether weight per unit length due to increased self weight. The payload capacity also decreases slightly with change in angle of attack. With reduction in angle of attack, fin sizes required are considerably high. The fin weight and the location of confluence point depend to a great extent, on the location of CG. Backward movement of the CG causes the fin size to decrease but moves the confluence point forward to an undesirable position.

## V. Summary and Conclusions

Most studies on aerostat envelope shapes are carried out on the basis of aerodynamic considerations. However, an aerostat being primarily a payload carrying device, its efficacy depends on its net payload carrying capacity. Aerodynamic analysis is carried out using a semi-empirical method. The Envelope drag at zero angle of attack is determined using a response surface. A methodology has been developed for sizing the fins of the aerostat. Methods to determine the weight of the tether to be carried by the aerostat have also been employed in order to study the effect of drag on the payload capacity of the aerostat. The shape generation algorithm proposed by Kanikdale et al.[1] has been made more robust by introducing a new constraint to avoid kinks and folds to develop on the shape. The payload of an aerostat of the GNVR shape has been estimated for a single fabric and multi-fabric construction. A 5 % decrease in envelope fabric weight was observed due to the multi-fabric construction. There was a 20% increase in payload capacity due to decrease in fin size. This was however obtained at the expense of moving the confluence point away from its desired position due to shift in the centre of gravity. Shapes have been generated using the shape generation algorithm and a GA based optimizer GADO used to determine the most optimum shape using single and multi-fabric construction. Sensitivity of the payload capacity of the aerostat to different operating conditions and design requirements has been studied.

## References

[1]Kanikdale, T. S., Marathe, A. G., and Pant, R. S., "Multidisciplinary Optimization of Airship Envelope Shape", AIAA-2004-4411, Proceedings of 10th AIAA/ISSMO Multidisciplinary Analysis and Optimization Conference, Albany, USA, 2004.

[2] Rasheed K. M., "GADO: A Genetic Algorithm For Continuous Design Optimization", Ph.D. Dissertation, Graduate School, New Brunswick Rutgers, The State University of New Jersey, January, 1998.

[3]Kale S. M., Joshi P., Pant R. S., "A Generic Methodology to Estimate Drag on an Aerostat Envelope", *Proceedings of AIAA 5th Aviation Technology, Integration, and Operations Conference (ATIO) and 16th Lighter-Than-Air Systems Technology Conference and Balloon Systems Conference*, September 2005, Arlington, USA.

[4]Wright J. B., Computer programs for tethered-Balloon System Design and Performance Evaluation, Report No. AFGL-TR-76-0195, Air Force Geophysics Laboratories (LCB) Hanscom AFB, Massachusetts 01731, August 1976.

[5]Krishnamurthy M., Panda G.K., “Equilibrium Analysis of a Tethered Aerostat”, Project document FE 9802, Flight Experiments division, National Aerospace Laboratories, November 1998.

[6]Jones S. P., Delaurier J. D., “Aerodynamic Estimation Techniques for Aerostats and Airships”, American Institute of Aeronautics and Astronautics, Report No. 81-1339, 1981.

[7]Gill P., Malik S., Pant R. S., “Estimation of Aerodynamic Characteristics of Un-Symmetrically Finned Bodies of Revolutions”, *Proceedings of 28$^{th}$ Fluid Mechanics & Fluid Power Conference*, Chandigarh, India, December 2001.